PFC/JA-83-42

Transport of Injected Impurities in Heliotron E

J. E. Rice, J. L. Terry, E. S. Marmar

Plasma Fusion Center
Massachusetts Institute of Technology
Cambridge, MA 02139

O. Motojima, H. Kaneko, K. Kondo, T. Mizuuchi,
S. Besshou, T. Mutoh, F. Sano, A. Sasaki, M. Sato,
S. Sudo, H. Zushi, M. Iima, K. Magome, T. Ohbiki,
A. Iiyoshi, K. Uo

Kyoto University Plasma Physics Laboratory
Gokasho Uji, Japan

December 1983

This work was supported by the U.S. Department of Energy Contract No. DE-AC02-78ET51013. Reproduction, translation, publication, use and disposal, in whole or in part by or for the United States government is permitted.

Transport of Injected Impurities in Heliotron E

J. E. Rice, J. L. Terry, E. S. Marmar

Plasma Fusion Center, M.I.T. Cambridge, MA 02139

and

O. Motojima, H. Kaneko, K. Kondo, T. Mizuuchi, S. Besshou, T. Mutoh, F. Sano, A. Sasaki, M. Sato, S. Sudo, H. Zushi, M. Iima, K. Magome, T. Ohbiki, A. Iiyoshi, K. Uo

Kyoto University Plasma Physics Laboratory

Gokasho Uji, Japan

Abstract

Impurities have been injected into Heliotron E in order to study the transport properties of currentless plasmas. In ECH produced plasmas, the impurity transport can be described by purely anomalous diffusion, with a coefficient of order a few thousand cm^2/sec. During neutral beam operation, the impurity transport can be characterized by considerably weaker diffusion and the presence of inward convection, with velocities as large as a few hundred cm/sec.

(1) Introduction

Impurities can play an important role in the production of reactor-grade plasmas, through radiation, enhanced resistivity and dilution of the working gas. Their presence may also affect the energy and particle tranpsort of the plasma. It is therefore necessary to understand the origins and subsequent transport of impurities in the plasma. While many

experiments have been performed in tokamaks[1,2,3,4,5,6,7,8,9] to determine the nature of impurity transport, very few direct measurements have been done on stellarators[10], heliotrons and torsatrons. There is considerable speculation that impurities are important in the overall dynamics of stellarator plasmas[10,11], especially during neutral beam heating experiments. It is the purpose of this study to try to determine the nature of impurity transport in machines that operate without plasma current.

Impurities have been injected into Heliotron E using the laser blow-off technique.[12] Heliotron E[13,14] is a non-axisymmetric $\ell = 2$ toroidal device (major radius = 2.2 m, average minor radius = 20 cm) with strong magnetic shear and a large rotational transform ($\iota(a_L) = 2.5$). For currentless plasmas, there are two basic operating modes: ECH produced plasmas formed by injecting up to 350 kW of power at 53.2 GHz into hydrogen and deuterium gases at a helical magnetic field of 1.9 T, and neutral beam heated plasmas created by injecting up to 2.2 MW of beam power into ECH discharges at helical fields of .94 and 1.9 T. The impurity emissions from injected silicon, titanium and iron were observed with two visible spectrometers, a 2.2m grazing incidence monochromator, a flat crystal Bragg spectrometer, an x-ray diode array, and two bolometer arrays. Parameter studies of impurity transport were performed by varying the electron density, the working gas, the input ECH and NBI powers, and the helical field during impurity injection.

(2) Transport in ECH plasmas

Shown in Fig.(1) are the time histories of emissions from several charge states of silicon, with the background subtracted, for injections into hydrogen ECH plasmas, with $\bar{n}_e = 8 \times 1012$ cm^{-3}, $T_e = 1000$ eV and T_i

≈ 200 eV. There is a rapid increase in all of the signals, which peak sequentially in time, followed by a more gradual decay back down to the pre-injection level. This indicates that for this type of discharge, the silicon leaves the plasma, and there is no accumulation, a situation reminiscent of some anomalous impurity transport in tokamaks[2,5,6]. Computer modelling[5] of this impurity transport indicates that these observations can be accounted for with only the effects of diffusion, shown by the dashed lines in Fig.(1) to compare with the individual ionization state emissions. In this particular case, the anomalous impurity diffusion coefficient required to match the time histories is 4500 cm^2/sec, constant in time and radius. Profile information is provided by an x-ray diode array, which is primarily sensitive to the 1s-2p transitions in helium-like silicon. Shown in Fig.(2) are x-ray brightness profiles at various times after the injection, with the background subtracted, for a silicon injection into a deuterium ECH discharge. Also shown are the calculated profiles from the impurity transport code, which includes measured temperature and density profiles, this time with a diffusion coefficient of 2000 cm^2/sec. An average minor radius, aL, of 20 cm was used in the calculations. The agreement of the code predictions and the observed time histories and profiles is suggestive that the anomalous impurity diffusion process observed in tokamaks is also at work in these Heliotron E ECH plasmas. These observations cannot be accounted for by pure neo-classical impurity transport due to collisions.

There are several similarities between the impurity transport in Heliotron E ECH discharges and the anomalous impurity diffusion in tokamaks, namely an increase in the impurity confinement time by about a factor of two in changing from hydrogen to deuterium[2,5,6] working

gases as shown from a comparison of Figs.(1 and 2), and the independence of impurity confinement on the mass of the injected impurity[5,6]. There was no observed difference in the decay times of injected silicon, iron and titanium in similar plasmas. Some new features of this anomalous impurity transport are that the diffusion coefficient is independent of ECH power, at least in going from 120 to 320 kW (here the electron temperature changed from 750 to 1100 eV), and that there is a possible dependence of transport on electron density, with longer impurity confinement at the higher densities.

The similarity between impurity transport in these ECH plasmas and the transport in clean, ohmically heated tokamaks can be further emphasized by comparing the Heliotron E observations to the anomalous impurity confinement time scaling law deduced in ref.(5). In order to make a direct comparison with eq.(5) of ref.(5), a value for the limiter safety factor, q_L, must be determined. This presents a problem since the q profile in Heliotron E has the opposite spatial dependence of that in a tokamak. Furthermore, q_L was not actually varied in the Alcator impurity injection experiments, only the plasma current and the toroidal magnetic field, and the impurity confinement time was found to scale as I/B_T. Since there was no plasma current or purely toroidal magnetic field in Heliotron E for these injection experiments, it would be convenient to replace I/B_T with another expression. If the temperature profile is gaussian shaped, then the characteristic 1/e width, a_T, for ohmically heated tokamak plasmas is proportional to the square root of I/B_T[15]. This allows the safety factor to be written $1.5\ a_L^2/a_T^2$, and the impurity confinement time scaling law becomes

$$\tau_I = .05\, m_{BG}\, a_T^2\, Z_{eff}\, R^{.75}/a_L \quad . \quad (1)$$

As was emphasized in ref.(5), the depedence on major radius, R, above cannot be taken too seriously, because in the Alcator C major radius scaling experiment, R was only varied between 57 and 71 cm. If 64 cm is used for R, and a temperature profile width, a_T, of 14 cm (consistent with Thomson scattering measurements) is taken, along with an average minor radius of 20 cm, and Z_{eff} = 1.5 for hydrogen plasmas, then the predicted impurity confinement time from Eq.(1) is 11 ms. This value is in excellent agreement with the 13 ms decay time deduced from the central charge states in Fig.(1).

The qualitative and quantitative agreement of injected impurity transport in Heliotron E ECH plasmas and in clean, ohmically heated tokamaks, indicates that the underlying anomalous impurity transport mechanism is independent of the magnetic field configuration (heliotrons, stellarators, torsatrons or tokamaks) or q profile, provided the heating is applied to the electrons.

(3) Transport in NBI plasmas

The situation is substantially different in neutral beam heated Heliotron E discharges. Shown in Fig.(3) are the time histories of sodium-, lithium- and helium-like silicon, with the no injection backgrounds subtracted, for an injection into a neutral beam heated hydrogen discharge, with $\bar{n}_e = 3.4 \times 10^{13}$ cm^{-3}, T_{eo} = 650 eV and T_{io} = 500 eV. In contrast to the ECH case, the two central states do not return to the pre-injection level within the duration of the discharge, and in fact the soft x-ray trace is still rising at the end of the shot. This indicates

that at least on this time scale, the injected impurities are accumulating. In order to match the impurity transport code predictions with the observed signals, a diffusion coefficient, D, of 600 cm^2/sec was required, in addition to an inward convection velocity, V, of 75 cm/sec. The calculated brightness time histories for helium- and lithium- like silicon are shown as the dashed curves in Fig.(3). In this particular case the parameter S ($\equiv V\ a_L/2D$)[16] was equal to 1.25. These values of D and S lead to a calculated[16] impurity confinement time, τ_I, of 190 msec. The necessity of the inclusion of an inward convection velocity to account for observed impurity transport has been seen in tokamaks[6,8,9,17] and stellarators[10]. In fact, transport coefficients of this size are similar to the neo-classical values, although quantitative agreement is not obtained between the observations and the code predictions when only the effects of neo-classical impurity transport are included.

The soft x-ray brightness profiles at several different times after an iron injection into a deuterium NBI plasma are shown in Fig.(4). For this case, the average electron density was 2.7×10^{13} cm^{-3} and the central electron temperature was 750 eV. A steady state condition was not attained during the discharge as the profile continuously became more peaked until the beams were turned off. In order to match the code predictions with these observations, a diffusion coefficient of 200 cm^2/sec and an inward convection velocity of 500 cm/sec (S = 25) were required. Again, the diffusion coefficient was taken to be independent of radius and time, and the convection velocity was taken to have the form $V\ r/a_L$, also static. In this case, the calculated τ_I is 2 years! The predicted x-ray traces, from 3d-2p transitions of Fe^{18+} to Fe^{23+}, are also shown in Fig.(4). The agreement is quite good.

This concentration of impurities appears to be stronger in deuterium NBI plasmas than in hydrogen in that the diffusion coefficient is smaller and the inward convection velocity is larger. There is some evidence that the inward flow of impurities is also stronger at higher electron densities, from a density scan in hydrogen NBI plasmas from 2.0×10^{13} $cm^{-3} < n_e < 7.0 \times 10^{13}$ cm^{-3}. The decay time of the lithium-like silicon brightness increased as the electron density was increased, and the soft x-ray signal became steady in time or even monotonically increased at the higher densities. This indicates that either the diffusion coefficient decreases or the convection velocity increases at higher electron densities. The transport in NBI plasmas is not strongly dependent on the impurity species, as injections of silicon, titanium and iron yield similar results.

There is, however, no unique picture which describes the transport in NBI plasmas. Seemingly similar discharges exhibit a large variation of diffusion coefficients and convection velocities necessary to account for the observations. In fact, there is evidence that these transport coefficients may vary in time during some discharges. This is in contrast to the ECH cases where there seems to be simple, consistent behavior.

(4) Conclusions

It is apparent from a comparison of impurity injections into ECH and NBI plasmas that the underlying impurity transport mechanisms are inherently different in the two cases. In ECH plasmas the transport seems to be purely anomalous diffusion, similar to that observed in some tokamaks[2,5,6]. In the NBI case, the transport appears to more like

neo-classical impurity transport, and in some instances, strong inward convection is seen. This sort of behavior has also been observed in tokamaks[9,17]. A fundamental difference between the two types of discharges is the recipient of the input power. ECH plasmas are similar to ohmic discharges in that the electrons are heated; the neutral beams couple directly to the ions, initially producing an excess of high energy ions. If, for instance, some of these high energy ions are not well confined, their loss from the plasma would create a radial electric field. This electric field could then cause an inward flow of thermal impurities, giving rise to impurity accumulation.

(5) Acknowledgements

The authors would like to thank Ron Parker for his encouragement with this program, Tomosumi Baba and Tohru Senju for assistance during the experiment and Jeff Harris for useful discussions.

References

(1) S. A. Cohen, J. L. Cecchi and E. S. Marmar, Phys. Rev. Lett. 35, 1507 (1975)

(2) E. S. Marmar, J. E. Rice and S. L. Allen, Phys. Rev. Lett. 45, 2025 (1980)

(3) S. Suckewer et al., Phys. Lett. 80A, 259 (1980)

(4) K. H. Burrell et al., Nucl. Fus. 21, 1009 (1981)

(5) E. S. Marmar et al., Nucl. Fus. 22, 1567 (1982)

(6) TFR Group, Phys. Lett. 87A, 169 (1982)

(7) S. Cohen et al., J. Vac. Sci. Technol. 20, 1226 (1982)

(8) TFR Group, Nucl. Fus. 23, 559 (1983)

(9) R. C. Isler et al., Nucl. Fus. 23, 1017 (1983)

(10) W VII-A Team, 11th Eur. Conf. on Contr. Fus. and Plas. Phys., Aachen, 195 (1983)

(11) W VII-A Team, IAEA-CN-41/L5, 9th Int. Conf. on Plas. Phys. and Contr. Nucl. Fus., Baltimore (1982)

(12) E. S. Marmar, J. L. Cecchi and S. A. Cohen, Rev. Sci. Instrum. 46, 1149 (1975)

(13) K. Uo et al., 10th Eur. Conf. on Contr. Fus. and Plas. Phys., Moscow (1981)

(14) K. Uo et al., 11th Eur. Conf. on Contr. Fus. and Plas. Phys., Aachen, 185 (1983)

(15) J. E. Rice, K. Molvig and H. I. Helava, Phys. Rev. A 25, 1645 (1982)

(16) F. H. Seguin, R. Petrasso and E. S. Marmar, Phys. Rev. Lett. 51, 455 (1983)

(17) G. Jahns et al., Nucl. Fus. 22, 1049 (1982)

Figure captions

1) Silicon injection into a hydrogen ECH plasma (solid lines), with code predictions (dashed curves).

2) Soft x-ray brightness profiles for silicon injection into a deuterium ECH plasma (top), with code predictions (bottom).

3) Silicon injection into a hydrogen NBI plasma (solid lines), with code predictions (dashed curves), as a function of time after the injection.

4) Soft x-ray brightness profiles (top), with the background subtracted, for iron injection into a deuterium NBI plasma, with code predictions (bottom).

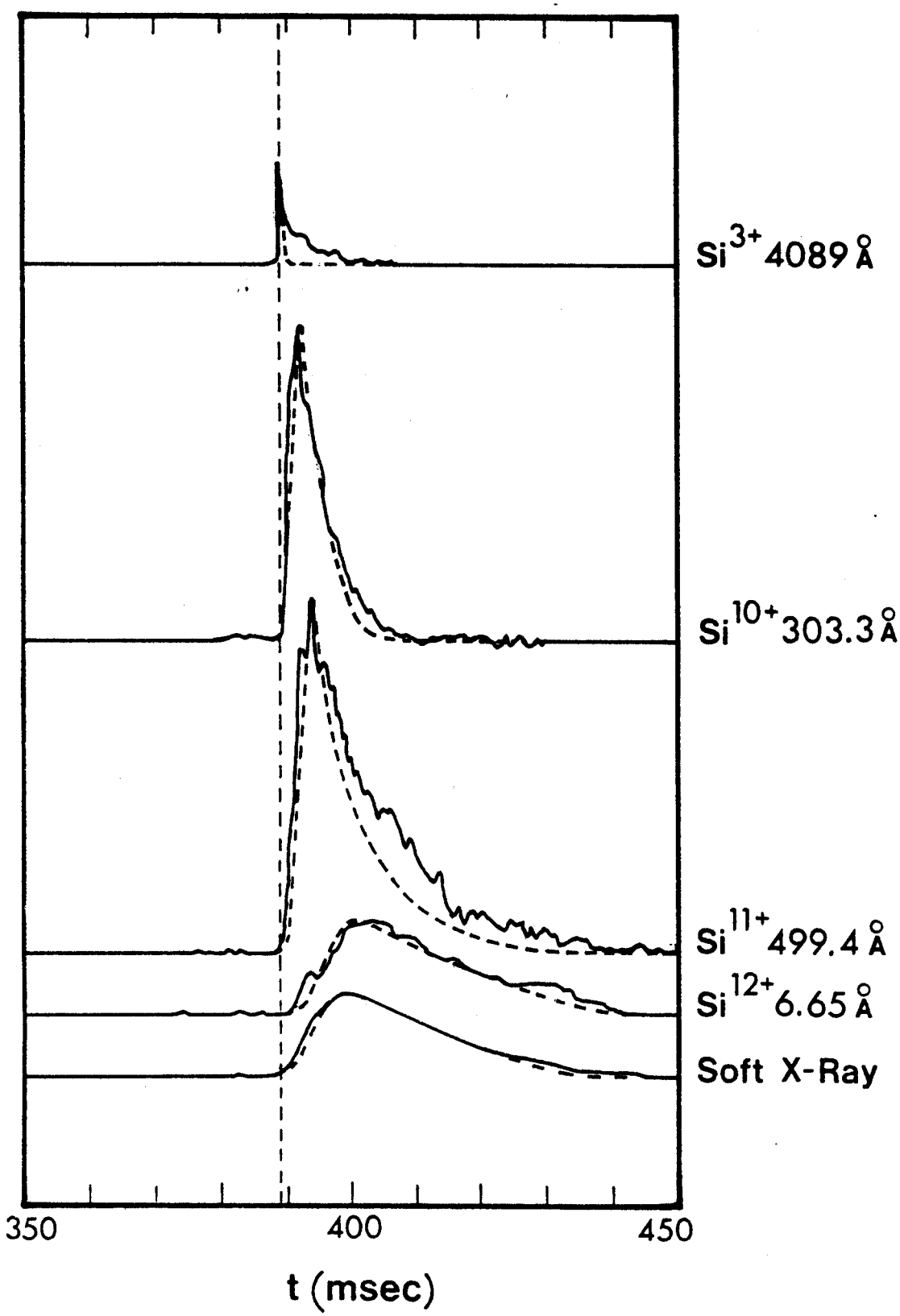
H_2
300 KW ECH
T_e=1000 eV
$\bar{n}_e=8\times10^{12}cm^{-3}$
D=4500 cm^2/sec
Si^{3+} 4089 Å
Si^{10+} 303.3 Å
Si^{11+} 499.4 Å
Si^{12+} 6.65 Å
Soft X-Ray
350
400
450
t (msec)

Figure 1

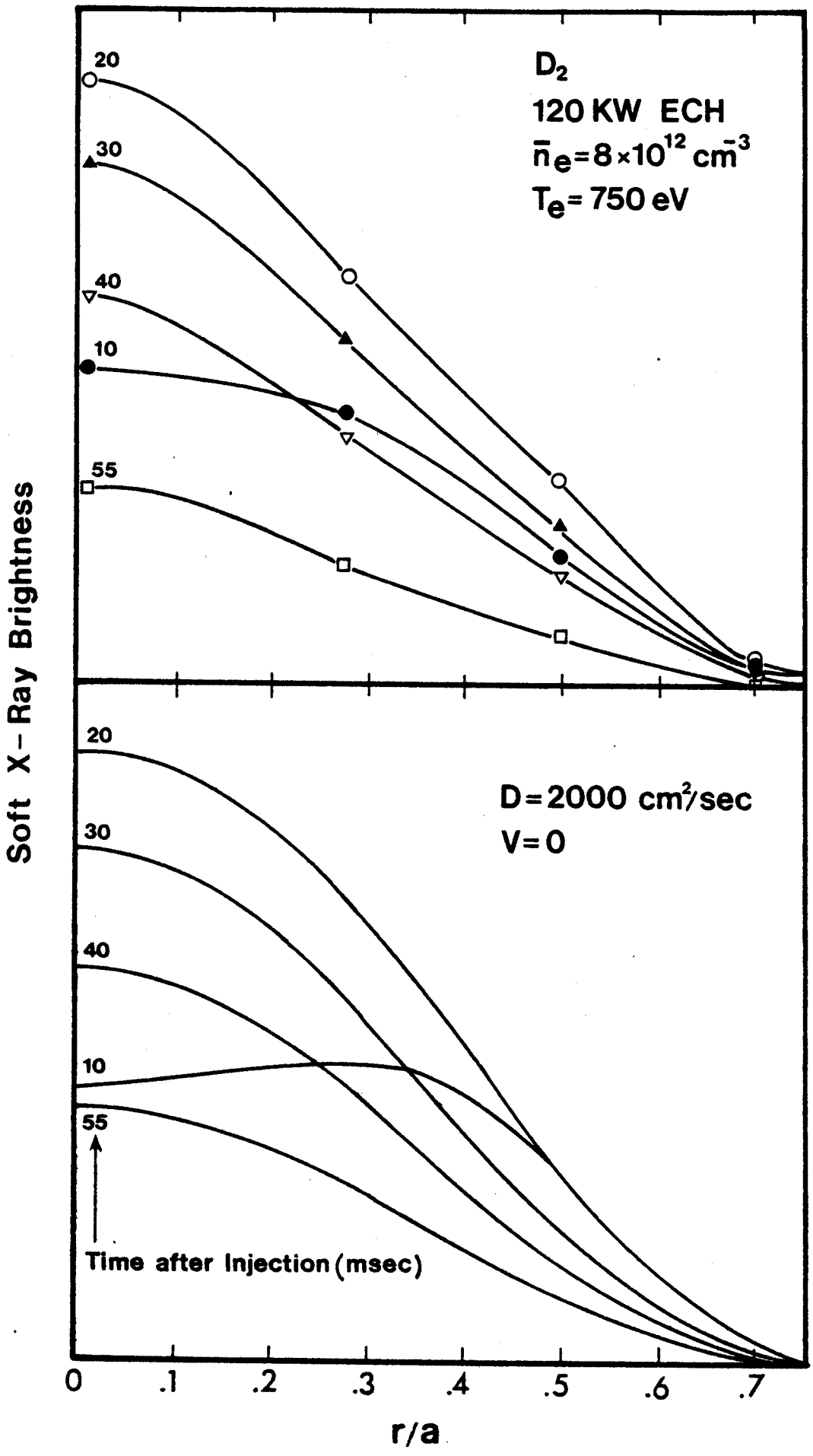
Soft X-Ray Brightness
20
30
40
10
55
D2
120 KW ECH
n̄e=8×10^12 cm^-3
Te= 750 eV
20
30
40
10
55
D=2000 cm²/sec
V=0
Time after Injection (msec)
0
.1
.2
.3
.4
.5
.6
.7
r/a

Figure 2

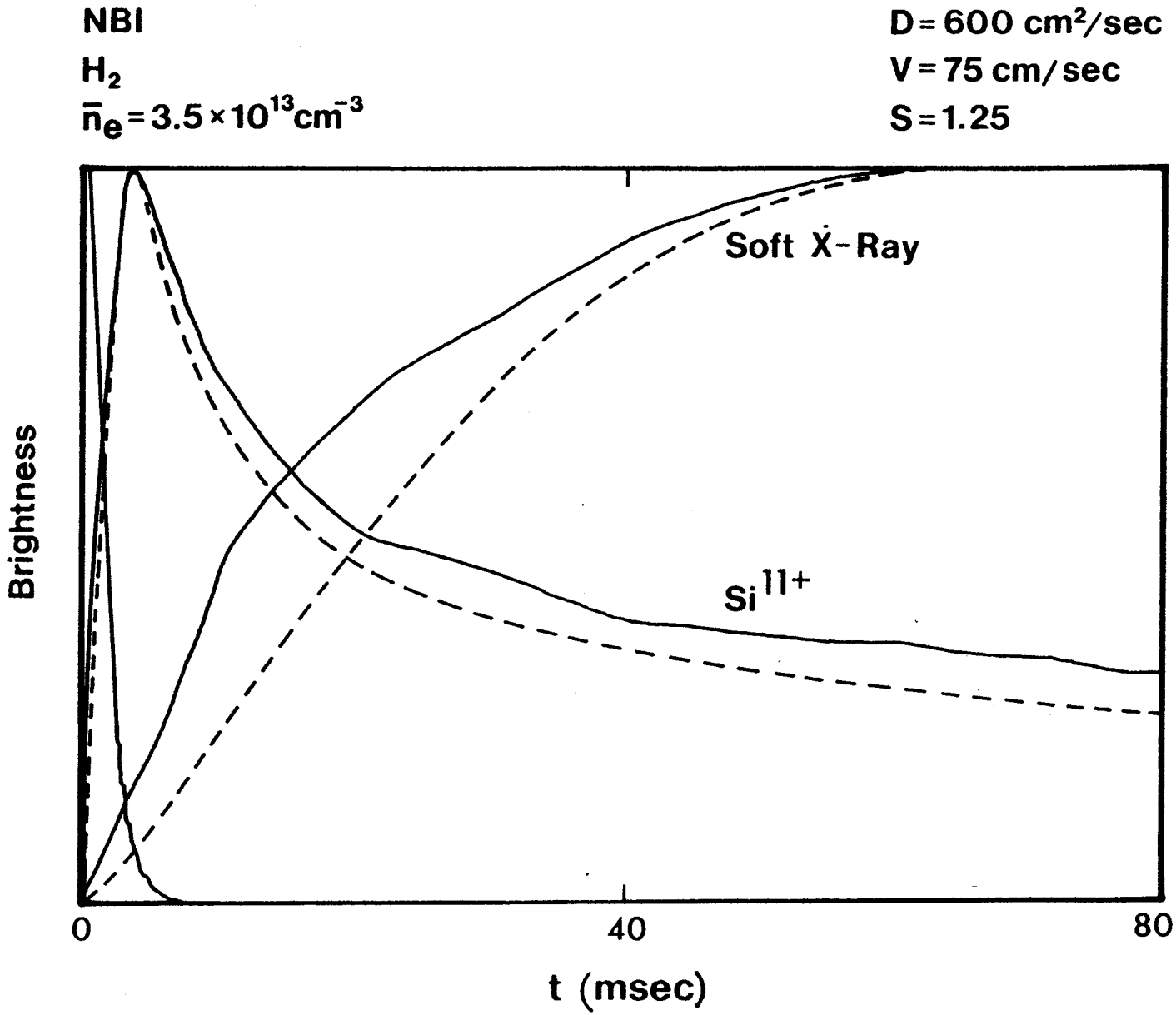
NBI
H_2
$\bar{n}_e = 3.5 \times 10^{13} cm^{-3}$
$D = 600\ cm^2/sec$
$V = 75\ cm/sec$
$S = 1.25$
Soft X-Ray
Si^{11+}
Brightness
0
40
80
t (msec)

Figure 3

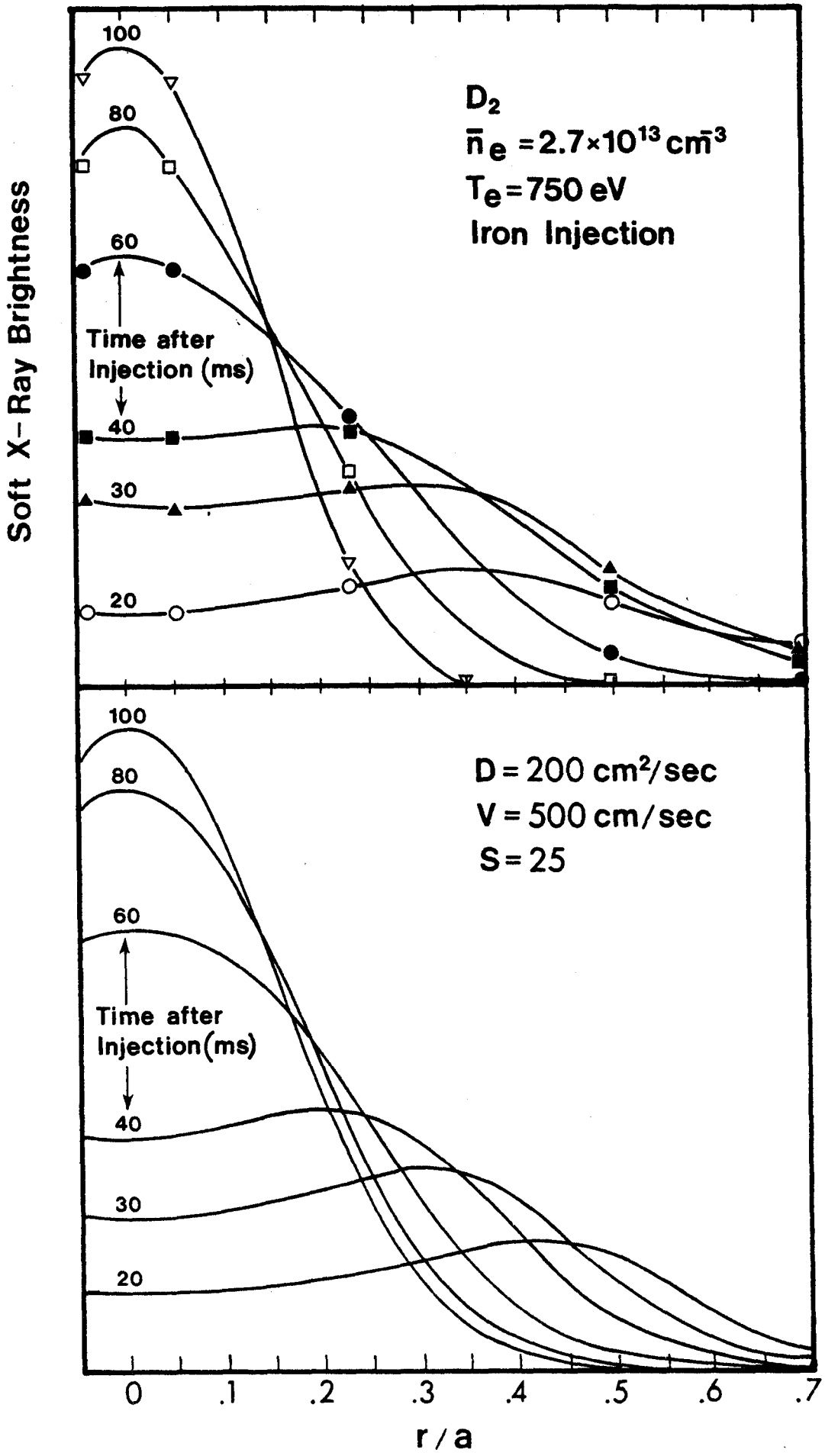
Soft X-Ray Brightness
100
80
60
Time after
Injection (ms)
40
30
20
D2
n̄e = 2.7×10^13 cm^-3
Te = 750 eV
Iron Injection
100
80
60
Time after
Injection(ms)
40
30
20
D = 200 cm²/sec
V = 500 cm/sec
S = 25
0
.1
.2
.3
.4
.5
.6
.7
r/a

Figure 4